OSP Journal of Nanomedicine and Nanotechnology

Research Article

Use of Cellulose Nanocrystals in Chitosan Nanoparticles Carrier System for the Controlled Release of Ketoprofen

Abo-Elseoud WS[1], Hassan ML[1,2], Sabaa MW[3], Basha M[4], Hassan EA[1], S M Fadel[1]

[1]*Cellulose and Paper Department & Advanced materials and Nanotechnology Group, Centre of Excellence for Advanced Sciences, National Research Centre, Dokki, Giza 12622, Egypt*
[2]*Egypt Nanotechnology Centre, Cairo University, El-Sheikh Zayed, 6th October City 12588, Egypt*
[3]*Chemistry Department, Faculty of Science, Cairo University, Giza 12613, Egypt*
[4]*Pharmaceutical Technology Department, National Research Centre, Dokki, Cairo 12622, Egypt*

Corresponding Author: Mohammad L Hassan, Cellulose and Paper Department & Advanced materials and Nanotechnology Group, Centre of Excellence for Advanced Sciences, National Research Centre, Dokki, Giza 12622, Egypt. E-mail: ml.hassan@nrc.sci.eg

Received: October 30, 2019; **Accepted:** January 13, 2020; **Published:** February 28, 2020

Abstract

This investigation aimed to use the cellulose nanocrystals and chitosan nanoparticles (CHNP) for developing controlled drug delivery systems of the non-steroidal anti-inflammatory drug Ketoprofen (KP). Cellulose Nanocrystals (CNC) were isolated from date palm stalks by sulfuric acid hydrolysis; the isolated nanocrystals had dimensions of 86-237 nm in length and 5-7 nm in width. Chemical modification of cellulose nanocrystals by oxidation to introduce carboxylic groups and by amine functionalization to introduce amino groups on their surface was also carried out. The effect of the chemically modified CNC on the controlling of Ketoprofen release was also investigated. The prepared systems containing CHNP and the different ratios cellulose nanocrytals showed high entrapment efficiency of ~ 73 - 80%. Addition of cellulose nanocrystals at different ratios to CHNP affected the KP release to different degrees depending on the kind of the nanocrystals used (non-modified, carboxylated or aminated). Particle size analysis showed that the addition of cellulose nanocrystals had no significant effect on the CHNP size. Compatibility studies by FTIR spectroscopy showed no chemical reaction between KP and the system's components used.

Keywords: Cellulose Nanocrystals; Chitosan Nanoparticles; Ketoprofen, Chemical Modification

Introduction

In the recent years, with a great advance of nanotechnology [1], new strategies have been developed for the preparation of composite Nanoparticles (NP) based controlled release drug delivery systems made of biocompatible and biodegradable materials [2]. Such systems have many advantages, which could not only protect the drugs from degradation, enhance drug solubility and control the rate of drug release to prolong the therapeutic duration, but also could achieve an effective drug delivery at the site of action [3].

Cellulose Nanocrystals (CNC), which are crystalline nanoparticles separated from cellulosic materials by acidic hydrolysis, play an essential role in the development of new biomaterials with enhanced properties. Cellulosic materials have a great tendency to form dense matrices when blended with other pharmaceutical excipients due to their excellent compaction properties, which is suitable for the oral drug administration. CNC was first reported as a drug excipient in the pharmaceutical formulations by Jackson and coworkers [4]. The negative charge beside the abundance of surface hydroxyl groups of CNC suggests that large amounts of drugs might bind to their surfaces with high payloads and optimal control of dosing [5]. Ionic interactions between the excipients and the drug can affect the drug release. Furthermore, there are numerous researches that proved the safety of CNC to be used in biomedical applications [6-9]. CNC have attracted a great attention in multiple applications such as drug delivery [10], regenerative medicine [11], tissue engineering [12] and so on [13-15]. Roman and coworkers suggested the use of CNC as carriers in targeted delivery of a variety of therapeutics [9]. Moreover, due to their antimicrobial properties, CNC could be used as antimicrobial agent in the preparation of wound healing gels and antiseptic solutions [16,17]. Zainuddin *et al*. used hydrophobically modified kenaf CNC as an excipient for hydrophobic drug Curcumin. CNC was modified with Cetyl Trimethylammonium Bromide (CTAB) as a cationic surfactant [18].

Chitosan is a modified natural cationic polysaccharide derived from the deacetylation of the naturally occurring chitin. It is the second abundant polymer next to cellulose [19,20] , which composed of N-acetylglucosamine and glucosamine residues. Due to its attractive properties such as biodegradability, biocompatibility, antimicrobial activity [21] and non- toxicity [22] in addition to its tendency for formation of nanoparticles, it was extremely used as a good candidate

polymer in designing of controlled release pharmaceutical formulations. Due to the availability of free amino groups in the chemical structure of chitosan, it carries a positive charge in acidic medium and thus, in turn, could react with many negatively charged polymers/surfaces. The bio adhesive and cationic nature of chitosan enhances the drug permeability and increases the residence time in the mucous which in turn increases the absorption of drugs from the mucosal membranes [23,24].

Ketoprofen (KP), [2-(3-benzoylphenyl) propionic acid], is an active component which widely used as Non-Steroidal Anti-Inflammatory Drugs (NSAID) to reduce inflammation, pain and stiffness caused by several conditions such as rheumatoid arthritis, osteoarthritis, abdominal cramps associated with menstruation or other various painful inflammatory states. Recently, it also has been used in the prevention of various cancers including lung and colorectal cancers as well as in treatment of some neurodegenerative disorders such as Alzheimer's disease and Parkinson's disease [25,26] . Ketoprofen is rapidly and completely absorbed from the gastrointestinal tract after oral administration, exhibiting a short half-life of 1-2 hs. Like other NSAIDs, Ketoprofen causes local adverse effects in gastrointestinal tract. Therefore, Ketoprofen is considered as a candidate for controlled drug delivery research due to its short half-life and poor solubility in water that affects its bioavailability [27,28].

Due to the integrated characteristics of both cellulose nanocrystals and chitosan nanoparticles, both of them could be exploited for developing a promising drug carrier for Ketoprofen. In the literature, many attempts have been developed to produce controlled release systems for Ketoprofen using carboxymethyl chitosan microparticles [29], chitosan nanoparticles [30], polycaprolacton microspheres [31], cellulose ether polymer mixtures (hydroxypropylmethylcellulose and hydroxypropylcellulose) [32] and cellulose acetate [33].

The current work is focused on the preparation and characterization of the chitosan nanoparticles/cellulose nanocrystals system prepared via ionic gelation using pentasodium Tripolyphosphate (TPP) as a crosslinking agent for the controlled release of KP. In a previous research, the same system was used for controlling the release of repaglinide with high entrapment efficiency producing good drug release profile suitable for use as anti-diabetic controlled release system [34].

In the current work, the prepared system containing ketoprofen was characterized using Transmission Electron Microscopy (TEM), Fourier Transform Infrared Spectroscopy (FTIR), surface charge, particle size analysis and evaluated regarding its entrapment efficiency of KP as well as the in vitro drug release behavior. Moreover, the effect of surface modification of CNC by TEMPO-oxidation and etherification with amine groups on the drug loading and the in vitro drug release was also investigated.

Materials and Methods

Raw materials

Ketoprofen were obtained from Amoun Pharmaceutical Company S.A.E., Egypt. Chitosan (low molecular weight grade, degree of deacetylation: 75-85%, viscosity: 20-300 cP in 1% acetic acid, average Mw ~ 50 kDa), pentasodium Tripolyphosphate (TPP), glacial acetic acid, hydrochloric acid (37%) and sulfuric acid (96-98%), 2,2,6,6-tetramethyl-1-piperidinyloxy (TEMPO) (98%), sodium hypochlorite (reagent grade, 10-15 % available chlorine) solution, sodium bromide (99.0 %), Epichlorohydrin (EPH), sodium hydroxide, ammonium molybdate, potassium iodide, sodium thiosulfate and methanol were purchased from Sigma-Aldrich. Ammonium hydroxide (NH_4OH 28-30 %), sodium hydrogen phosphate, potassium di-hydrogen phosphate of laboratory grade were obtained from Fluka and used without further treatment.

Date palm stalks pulp preparation

Date palm stalks were collected from local farms in Giza, Egypt. The pulp was prepared and bleached as previously described (35). It was washed with water and cut into 1-3 cm long, then, the palm stalks pulp was prepared by alkali treatment using 15% NaOH (w/w, based on oven-dried stalks) at 150 °C for 3h. The produced pulp was bleached using sodium chlorite/acetic acid mixture at 80 °C for 1h. Chemical composition of the bleached pulp was determined according to the previously published method [36], and was: alpha-cellulose contents 51.6%, hemicelluloses (as pentosans) 22.8%, ash content 2.3%, and ethanol/toluene extractives 1.7%.

Preparation of cellulose nanocrystals

Cellulose nanocrystals were prepared by sulfuric acid hydrolysis of the resultant bleached pulp (Hassan *et al*., 2014). The pulp was hydrolyzed by stirring in 65 wt. % sulfuric acid (20 mL/g cellulose) at 45 °C for 45 m. The hydrolysis was stopped by diluting the reaction mixture 10-fold with cold (~ 4 °C) deionized water. The nanocrystals were washed three times with deionized water and collected by centrifugation for 10 minutes, and then dialyzed (Spectra/Por 4 dialysis tubing) against water until the pH of fresh dialysis medium stayed constant over time. The nanocrystals suspension was sonicated for 6 m at 200 W under ice-bath cooling using ultrasonic processor (Kesheng Sonic, Vibra Cell (Ningbo Kesheng ultrasonic equipment Co., Ltd)).

TEMPO-mediated oxidation of CNC (OXCNC)

Surface oxidation of cellulose nanocrystals was performed according to the previously reported procedure [37]. CNC (1.94 g, 4 mmol glycosyl units) was dispersed in water (150 ml) and sonicated (Kesheng Sonics, Vibra Cell) for 10 m. Then, TEMPO (195 mmol) and NaBr (600 mg, 5.7 mmol) were added to the CNC suspension and stirred for 30 m at room temperature. The pH of the solution was 5.8, and adjusted to 10 by adding 0.5 M NaOH. The TEMPO-mediated oxidation of CNC was initiated by slowly adding NaOCl 13 % (14.7 ml, 20.4 mmol) over 20 m under gentle agitation. The reaction pH was kept constant at 10, by the continuous addition of 0.5 M NaOH. The reaction was known to be completed when no additional reduction in the pH was observed, over duration of 4 hours. Once the reaction was completed,

excess oxidant was quenched using methanol (15 ml) and the pH was adjusted to 7 using 0.5 M HCl. In order to purify the oxidized nanocrystals, the solution was dialyzed against water for at least 48 h.

Preparation of CNC amine (ACNC)

First, the CNC surface was decorated with epoxy functional groups via reaction with epichlorohydrin (6 mmol g^{-1} cellulose) in 1 M sodium hydroxide at 60 °C (132 mL/g cellulose) according to the method by Porath and Fornstedt [38]. After 2 h, the reaction mixture was dialyzed (Spectra/Por 4 dialysis tubing) against distilled water until the pH was below 12. Next, the epoxy ring was opened with ammonium hydroxide to introduce primary amino groups. After adjusting the pH to be 12 with 50% (w/v) sodium hydroxide, ammonium hydroxide (29.4%, 5 mL g^{-1} cellulose) was added and the reaction mixture heated to 60 °C for 2 h. The reaction mixture was dialyzed until the pH was 7.

Preparation of KP-CHNP/CNC nanocomposites

Ketoprofen loaded CHNP formulations containing different ratios of CNC, OXCNC or ACNC were prepared as shown in Table 1. CHNP/CNC, CHNP/OXCNC and CHNP/ACNC nanocomposites were prepared via the ionotropic gelation method [39]. Low molecular weight chitosan was dissolved in acetic acid 1% (w/v) and kept under magnetic stirring until complete dissolution. CNC, OXCNC or ACNC were added to the chitosan solutions in different ratios and stirred until formation of homogeneous mixture. KP (100 mg) was dissolved in 2 ml methanol and drop wisely added to the chitosan/cellulose nanocrystals mixture. Gelation was then carried out by adding 55 ml TPP (0.2%) to the mixture drop wisely; the pH was 4.5. The gelation process was carried out under constant magnetic stirring (500 rpm) at room temperature. The KP-loaded CHNP/CNC, CHNP/OXCNC or CHNP/ACNC nanoparticles were collected by centrifugation at 10,000 rpm, washed repeatedly by distillated water, dialyzed against distilled water using Spectra/Por 4 dialysis tubing until the pH of fresh dialysis medium remained constant over time. The purified nanoparticles were stored in screw-capped glass containers for further examination.

Table 1. Composition of KP-loaded CHNP/CNC, CHNP/OXCNC or CHNP/ACNC nanocmposites.

Formulation code	Chitosan	CNC	OXCNC	ACNC
	%	%	%	%
CHNP/CNC**(0%)-F1**	100	0	----	----
CHNP/CNC**(2.5%)-F2**	97.5	2.5	----	----
CHNP/CNC**(5%)-F3**	95	5	----	----
CHNP/CNC**(10%)-F4**	90	10	----	----
CHNP/CNC**(20%)-F5**	80	20	----	----
CHNP/OXCNC**(2.5%)-F6**	97.5	----	2.5	----
CHNP/OXCNC**(5%)-F7**	95	----	5	----
CHNP/OXCNC**(10%)-F8**	90	----	10	----
CHNP/OXCNC**(20%)-F9**	80	----	20	----
CHNP/ACNC**(2.5%)-F10**	97.5	----	----	2.5
CHNP/ACNC**(5%)-F11**	95	----	----	5
CHNP/ACNC**(10%)-F12**	90	----	----	10
CHNP/ACNC**(20%)-F13**	80	----	----	20

X-ray powder diffraction

The crystallinity of the CNC, OXCNC, ACNC, CHNP, KP/CHNP, KP-CHNP/CNC, KP-CHNP/OXCNC and KP-CHNP/ACNC were studied by X-ray diffraction (XRD) using X-ray diffractometer (PANalytical, Netherlands) at room temperature with a monochromatic CuKα radiation source (λ = 0.154 nm) in step-scan mode with a 2θ angle ranging from 4° to 50° with a step of 0.04 and a scanning time of 5 m. Crystallinity index (CrI) of cellulose nanocrystals were calculated using the following equation [40]: $CrI = (I_{002}-I_{am})/I_{002}$, where I_{002} is the intensity in the diffraction profile at the position of 002 peak (2θ = 22°) and I_{am} is the intensity at about 2θ = 18°.

Transmission electron microscopy (TEM)

Transmission electron microscopy of the prepared CNC, OXCNC, ACNC, KP-CHNP/CNC, KP-CHNP/OXCNC, and KP-CHNP/ACNC formulations was carried out using a JEOL 1230 transmission electron microscope (Japan) with acceleration voltage 100 kV. A drop of cellulose nanocrystals or formulation suspensions was used on a copper grid bearing a carbon film.

Carboxylic groups' determination

The carboxylic groups' content of the oxidized CNC was determined by acid-base titration following the procedure developed for the conductometric titrations (Habibi *et al*., 2006). In this procedure, TEMPO-oxidized CNC samples (50 mg) were suspended into 0.01 M hydrochloric acid (HCl) solutions (15 mL) with stirring. The resulting suspensions were then titrated against 0.01 M sodium hydroxide (NaOH) solution.

Elemental Analysis

Elemental analysis for carbon and nitrogen was determined using Vario El Elementar (Germany), Elemental Analyzer.

Fourier transform infrared (FTIR) spectroscopy

FTIR spectra were acquired by a JASCO FTIR Spectrometer (FT/IR-6100) using KBr disc technique.

Zeta Potential (ZP) and Particle Size (PS) determination

Mean hydrodynamic ZP, PS and Poly-Dispersity Index (PDI) measurements were performed for CNC, OXCNC, ACNC, CHNP/CNC, CHNP/OXCNC and CHNP/ACNC formulations at a temperature of 25±0.1 °C using a Nicomp 380 ZLS dynamic light scattering (DLS) instrument (PSS, Santa Barbara, CA, USA), using the 632 nm line of a He Ne laser as the incident light with angel 90° and Zeta potential with external angel 18.9°.

Determination of entrapment efficiency (EE %)

The entrapment efficiency was determined by measuring the concentration of free KP in the suspension. The samples were centrifuged at 10,000 rpm for 20 m. The amount of free KP was determined in the supernatant by UV spectrophotometer at 259 nm. Supernatant of unloaded nanoparticles was used as basic correction. The entrapment efficiency could be calculated by the following equation (1) [41].

$$EE\ (\%) = [(W_{initial\ drug} - W_{free\ drug})/W_{initial\ drug}] \times 100 \quad (1)$$

In vitro release study

The release of KP from the prepared KP-loaded formulations compared to the free KP was carried out using the dialysis bag diffusion technique and phosphate buffer, pH 7.4. The samples containing 20 mg KP were placed in 500 ml of phosphate buffer at 37 ±0.5 °C for 8 h using shaking water bath. At fixed time intervals, 5 ml of samples were withdrawn and replaced by fresh medium to maintain constant volume. Samples were analyzed for amount of KP released by UV spectrophotometer at 259 nm.

Results and Discussion

Characterization of cellulose nanocrystals

TEM and XRD of CNC, OXCNC and ACNC

CNC, OXCNC and ACNC isolated from date palm stalks were characterized using TEM and XRD. TEM images (Figure 1a) of CNC isolated from date palm stalks showed that CNC had dimensions range of 86-237 nm in length and 5-7 nm in width. TEM images showed that the oxidation and modification of CNC with amine had no significant effect on the CNC dimensions; OXCNC were 78-200 nm and 5-6 nm in length and width, respectively, while, ACNC were 100-220 nm in length and 7-10 nm in width. These results agree with the previous studies of Habibi et al. who studied the oxidization of tunicate nanocrystals, and found that the TEMPO oxidation had no significant effect on the CNC dimensions [37]. The content of carboxylic groups of OXCNC was determined as 0.62 mmol g^{-1}, while that of CNC was determined as 0.015 mmol g^{-1}. Modification of CNC with amine also had no effect on the CNC dimensions and these results in accordance with the previously published studies followed the same method of preparation [42]. ACNC was synthesized by a simple and mild two-step reaction avoiding the use of protecting groups and so minimized the number of steps required for the preparation.

CNC had the XRD pattern of the known cellulose I crystalline structure which characterized with the two major peaks of 2θ centered at 23° and 15°, and another lower intensity peak at 2θ of about 34° (Figure 1b) [43]. Crystallinity index (CrI) of CNC, OXCNC and ACNC was 0.78, 0.77 and 0.84 respectively (Figure 2b). Oxidation and amination had no effect on the XRD diffraction pattern of CNC. Different studies in literature confirmed these obtained results [44,37]. This indicated occurrence of the reaction mainly at the surface of the nanocrystals.

Elemental Analysis of ACNC

To prove the modification of CNC surface with amine, the elemental composition of CNC and ACNC was determined. Nitrogen content of unmodified CNC was nil, while that of ACNC was 1.047 %, which confirmed the modification of CNC surfaces with amine groups. In addition, an increase in the carbon contents of CNC from 39.93 % to 45.86 % as a result of introduction of the substituent $-CH_2-CH(OH)-CH_2-NH_2$ onto the CNC surface. Sulfur content decreased from 0.48 to 0.108, this may be due to the hydrolysis of some of the sulfate ester groups at basic conditions during the modification reaction. The nitrogen content can be also used for the determination of the degree of surface substitution by Equation 2 [45].

$$DS = 162W/100M - [(M-1)W] \qquad (2)$$

Where W is the weight or weight percent in this case and M is the molecular weight of the substituent. The DS of resultant ACNC was calculated as 0.019. This value is close to that of previously published data on modification of CNC with amine functional groups by the same reagent used in this work (DS=0.02) [7].

FTIR spectra of cellulose nanocrystals

The TEMPO oxidation of CNC and their modification with amine were also confirmed by FTIR spectroscopy (Figure 1c). The CNC had a spectrum showed the characteristic peaks as the same that of cellulose, a broad band between 3000-3700 cm^{-1} attributed to the O–H stretching vibrations, band between 2800-3000 cm^{-1} is due to the aliphatic $-CH_2$ and –CH stretching vibrations. The peak at 1640 cm^{-1} attributed to the adsorbed water, peaks at 1425 cm^{-1}, 1158 cm^{-1} and 1064 cm^{-1} are for the stretching vibrations of C–O of the glycosidic bonds, and that of the primary and secondary hydroxyl groups, respectively. The out-of-plane deformational vibration peaks of the –OH groups appeared between 895 and 440 cm^{-1} [46]. FTIR spectrum of OXCNC confirmed the TEMPO oxidation of CNC by the appearance of the characteristic peak for the carboxyl groups at 1725 cm^{-1} in their acid form [37]. A small shift of the O–H stretching vibrations broad band was also found to be from 2900-3800 cm^{-1} attributed to the oxidation of the –OH groups at C_6 to carboxylic acid groups. Modification of CNC with amine can be also confirmed by the appearance of two interfering bands of primary amine at 3440 cm^{-1} and 3349 cm^{-1}. These two peaks interfered with the hydroxyl group broad band appeared between 3000-3700 cm^{-1}. The presence of amine was also confirmed by a medium peak appeared at 1070 cm^{-1} due to the stretching vibrations of C-N [47].

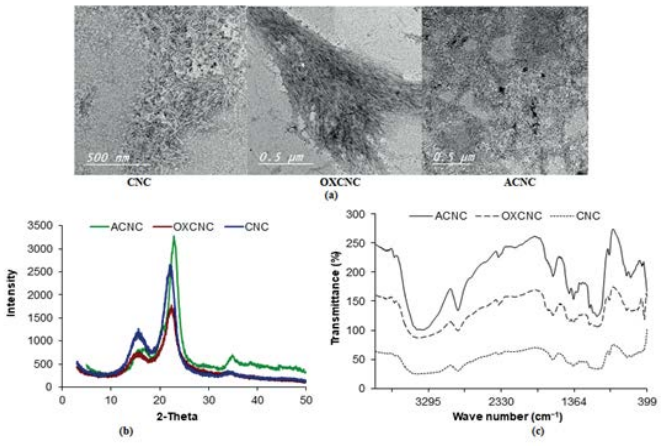

Figure 1. (a) TEM images, (b) XRD patterns, and (c) FTIR spectra of CNC, OXCNC and ACNC extracted from date palm stalks.

Zeta potential of cellulose nanocrystals

Cellulose nanocrystals used in this study had a high negative zeta potential of – 53.8 mV due to the presence of sulfate ester ($–OSO_3^-$) groups that incorporated during cellulose hydrolysis using sulfuric acid (Table 2). Zeta potential for the unmodified and modified CNC was measured at pH 6 (the pH of sulfuric acid treated CNC [48]. At this pH, OXCNC in the acid form, and the negative charge was mainly due to the presence of sulfate ester groups only. Azzam *et al*. reported reduction in the net surface charge of cellulose nanocrystals after TEMPO-oxidation, and they attributed that to the hydrolysis of sulfate ester groups at basic conditions during the oxidation reaction [49]. This explains the smaller measured zeta potential of OXCNC than that of CNC to be – 44.5 mV. At pH 6, $–NH_2$ groups of ACNC are partially protonated and carry positive charge which can electrostatically interact with some of negative sulfate ester groups leading to less net negative charge on the CNC amine surface to be – 38.7 mV. In addition, the use of basic medium during the modification with amine derivatives may cause the hydrolysis of some of the sulfate ester groups; this was confirmed from the decreasing of sulfur content in the elemental analysis.

Table 2. Zeta potential of cellulose nanocrystals.

Cellulose nanocrystals	ZP (mV)
CNC	– 53.8
OXCNC	– 44.5
ACNC	– 38.7

Characterization of Ketoprofen-loaded CHNP/CNC, CHNP/OXCNC and CHNP/ACNC nanocomposites

Entrapment Efficiency (EE %) of KP-loaded formulations

Table 4 shows the entrapment efficiency of KP into the CHNP, CHNP/CNC, CHNP/OXCNC and CHNP/ACNC nanocomposites. 100 mg of KP were dispersed in chitosan solution containing cellulose nanocrystals, and then gelation was carried out by adding 55 ml of 0.2% TPP. The results indicated the higher EE % of CHNP/KP ~ 79.78 ±2.11 %, while that of KP-CHNP/CNC formulations ranged between 73.61 ±3.45 – 78.31 ±3.15 %, KP-CHNP/OXCNC formulations ranged between 72.63 ±4.37 – 74.95 ±2.76 %, and KP-CHNP/ACNC formulations were 74.58 ±2.39 – 76.32 ±2.53%. Addition of the different cellulose nanocrystals to the chitosan nanoparticles formulations had no remarkable effect on the mean results of EE% of KP according to the close values of standard deviations. High entrapment efficiency of KP may be due to the stronger hydrogen bonding between the KP and both of chitosan and the different cellulose nanocrytals, in addition to the electrostatic attraction between the negatively charged cellulose nanocrystals and positively charged chitosan.

In-vitro release studies of KP-loaded formulations

Ketoprofen-loaded CHNP formulations were prepared via the ionic gelation method using TPP as a crosslinking agent at room temperature. The chitosan nanoparticles were formed by an electrostatic interaction of the positively charged amine groups of chitosan with the negatively charged phosphate groups of TPP [50]. This interaction created a stable matrix that might facilitate the entrapping of KP and render its release back from the matrix [51].

In order to assess the controlled release potential of KP-loaded nanocomposites, the *in-vitro* release of KP from the different formulations was performed. The release experiment was performed for 8 hours in phosphate buffer of pH 7.4. As depicted from Figure 2, the free KP exhibited faster release profile, where 99.84 % of free KP was released after 2 h compared to (30.67 - 49.52 %) of the KP released from the different formulations after two hours. Addition of the different cellulose nanocrystals (CNC, OXCNC, or ACNC) to the CHNP formulations significantly affected KP release. CHNP sample (without CNC) showed faster KP release profile (70.21%) compared to that having different amounts of CNC (40.82 - 45.96%), at the end of the release experiment. KP/CHNP samples having 2.5% and 20% CNC represented by **F2** and **F5**, had a sustained KP release profile of 45.96% and 40.82%, respectively at the end of the release experiment. Increasing the CNC concentration slightly decreased the KP release rate (Figure 2a). The lower rate of release in case of presence CNC could be due to physical hindrance of KP release by the rod-like CNC network formed. In addition, hydrogen bonding between the hydroxyl groups at the surface of CNCC and carboxylic groups of KP (Figure 3) could also retard release of the later.

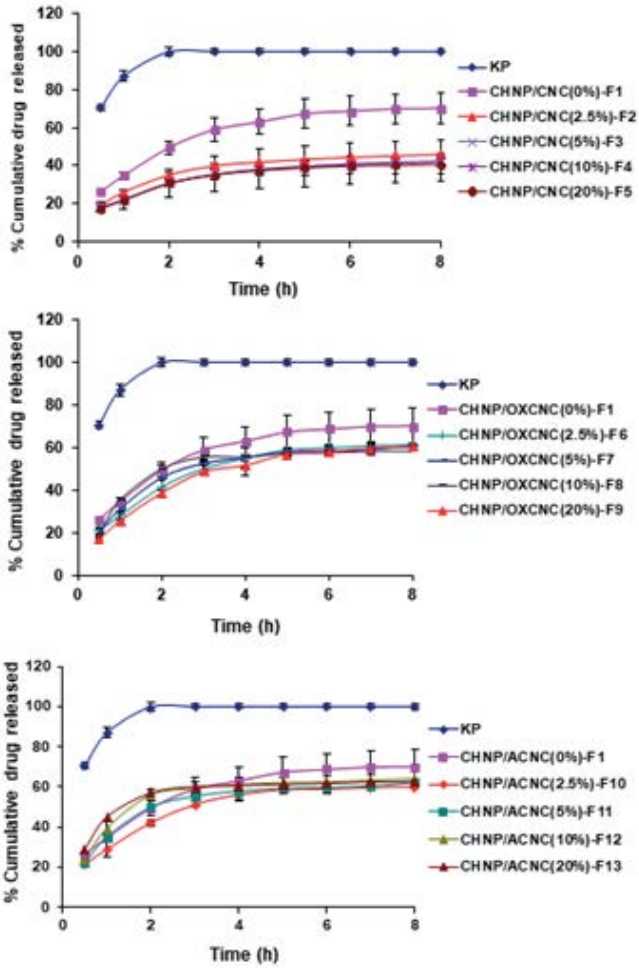

Figure 2. *In-vitro* release profiles of KP from (a) KP-CHNP/CNC, (b) KP-CHNP/OXCNC and (c) KP-CHNP/ACNC formulations.

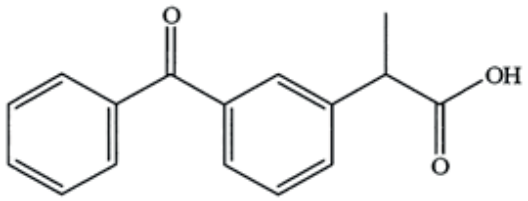

Figure 3. Chemical structure of Ketoprofin.

CHNP/OXCNC and CHNP/ACNC formulations showed a slower KP release profiles than that of neat CHNP (without CNC) by about 10%, while the CHNP/CNC formulations showed a slower release profiles than that of neat CHNP by about 30%. CHNP formulations containing different amounts of OXCNC had a KP release % range of (58.45 - 61.82 %), while that containing different amounts of ACNC had a KP release % range of (60.11 - 64.2 %), at the end of release experiment. Also, increasing the concentration of OXCNC and ACNC had no significant effect on the KP release (Figure 2b, c).

The slower release of ketoprofen in case of using CNC than ACNC could be due to stronger hydrogen bonding with carboxylic groups of KP in case of CNC than in case of ACNC due to higher electronegativity of oxygen of hydroxyl groups of CNC than nitrogen of amino groups of ACNC. In case of OXCNC, although stronger hydrogen bonding was expected between carboxylic acid groups of both OXCNC and KP than that between CNC and KP but the release of KP was faster in case of using OXCNC. This means that the primary hydroxyl groups at C6 (CH_2OH) are more readily available for hydrogen bonding with KP than the carboxylic groups of OXCNC.

Comparison between the different previously reported KP-loaded chitosan micro- and nanoparticles-based systems and the TPP-crosslinked chitosan system used in the current work is shown in Table 3 regarding the entrapment efficiency of Ketoprofen and its *in-vitro* release. As clearly shown in the table, the TPP-crosslinked chitosan nanoparticles in the current work showed higher entrapment efficiency and, at the same time, better KP release profile similar to other more complicated systems shown in the table. The closest entrapment efficiency to the formulations of the current work was that reported by Hardi *et al.* (76 - 89 %) (30), using TPP-crosslinked chitosan/oleic acid system. Nevertheless, the current work system sustained the KP release more than the system used in that study (93 - 99 % after 6 h, pH 7.4). This in addition to the nature sources, abundance and low cost of CNC more than oleic acid, made the system of the current work have better properties. Sugita *et al.* also used the same system of Hardi and obtained a close result of entrapment efficiency to that of Hardi and the current work (70 – 87 %), but not studied the *in-vitro* release [52]. Sugita *et al.* in other work used TPP-cross-linked chitosan/alginate system and obtained a close result of EE% to that of the current work (54-80%), but with a faster *in-vitro* release profile (90 %, after 3 h at pH 7.4) [53] Chimsook used chitosan/poly(ethylene glycol), (PEG) system with the resulted EE% of (52 - 73 %), and release profile of (82 - 98 %), after 12 h at pH 7.2; Chimsook used organic solvents to prepare this system. The polymer mixture of chitosan and PEG was dissolved in a mixture of dichloromethane and ethanol (1:1) with a vigorous stirring to form uniform drug polymer dispersion. Then the floating microspheres were obtained by dropping the polymer mixture into sodium lauryl sulfate solution (0.2%) at tempreture of 20 °C [54]. On the other hand, the current work used simple method without using organic or toxic solvents, in addition to the natural sources and abundance of the components, resulted in high EE% reached to ~ 80% and good drug release profile at pH value of 7.4 due to the open structure of the prepared formulations as a result of the presence of TPP crosslinks between the chitosan chains (Table 3).

Zeta Potential (ZP) and Particle Size (PS) determination of KP-loaded nanocomposites

ZP and PS of Ketoprofen-loaded CHNP/CNC, CHNP/OXCNC and CHNP/ACNC formulations were determined. As mentioned above, the chitosan nanoparticles were prepared by ionic gelation method and formed at pH 4.5, therefore the formed particles were positively charged. This was confirmed by the zeta potential measurements (Table 4). Addition of CNC, OXCNC and ACNC had no significant effect on the CHNP charge. Most of the samples had a slight increased ZP than that of CHNP itself with unloaded KP drug; otherwise those contained 20% CNC, 20% OXCNC, 20% ACNC had a closed value to this of unloaded CHNP as shown in Table 4. This may be due to the high negative charge of CNC, OXCNC and ACNC at this concentration, and some of their negative charge may be used to neutralize some of the increased charge due to the KP addition, in addition to their higher amounts in these samples.

Addition of KP, CNC, OXCNC and ACNC had no significant changes on the particle size measurements of CHNP. Slight increase in the PS of CHNP was observed upon addition of KP drug. This emphasized the nanostructure of KP that entrapped between the chitosan chains. High standard deviations were observed in the PS results of the studied KP-loaded CHNP formulations, this may be due to the disordered entrapment of the different cellulose nanocrystals rods inside the CHNP, which could rendered the direct diffusion of the dissolved KP through the CHNP matrix and sustained its release. PDI values of all the studied KP-loaded CHNP formulations were lower than 0.5 that indicated the high particle homogeneity [61].

TEM images of KP-loaded nanocomposites

TEM images of KP/CHNP, and some selected samples of KP-CHNP/CNC, KP-CHNP/OXCNC and KP-CHNP/ACNC-loaded with 100 mg KP are shown in Figure 4. The images showed the spherical geometry structure of the prepared particles and confirmed their nano-size. Slight changes in diameter of CHNP as a result of adding KP, CNC, OXCNC or ACNC were generally in agreement with the particle size analyses mentioned above. The diameter of the nanoparticles seen in the images ranged from about 150 to 400 nm for the different samples. The larger diameter of nanoparticles than those obtained from particle size analysis could be due to coagulation of the nanoparticles when they dry on the grid used for TEM images.

Table 3. Comparison of entrapment efficiency and release of Ketoprofen from chitosan micro- and nanoparticles-based drug delivery systems.

System	EE (%)	KP release (%)	Reference
TPP-crosslinked chitosan/CNC	74-80	~ 41-46 (after 8h, pH 7.4)	Current work
TPP-crosslinked chitosan/OXCNC	73-75	~ 58-61 (after 8h, pH 7.4)	Current work
TPP-crosslinked chitosan/ACNC	75-77	~ 60-64 (after 8h, pH 7.4)	Current work
N-benzyl-N,O-succinyl chitosan polymeric nanoparticles	70	Not studied	-55
Chitosan/Poly(N-Vinylcaprolactam-Co-Itaconic Acid-Co-Ethylene Glycol Dimethacrylate) microparticles	57	45-69 (after 48 h, pH 7.4)	-56
Glutaraldehyde or genipin crosslinked chitosan/poly(3-hydroxybutyrate) microparticles	52-62	20-70 (after 8 h, pH 7.4) 75-85 (after 72 h, pH 7.4)	-57
TPP-crosslinked chitosan/oleic acid nanoparticles	70-87	Not studied	-52
TPP-crosslinked chitosan/oleic acid nanoparticles	 76-89	14-17(after 3 h, pH 1.2) 93-99(after 6 h, pH 7.4)	-30
TPP-crosslinked chitosan/alginate nanoparticles	54-80	40 (after 3 h, pH 1.2) 90 (after 3 h, pH 7.4)	 -53
Chitosan/poly(ethyelenglycol) microspheres	52-73	82-98 (after 12 h, pH 7.2)	-54
TPP-crosslinked chitosan/poloxamer 188 nanoparticles	50	Not studied	-58
TPP-crosslinked β-cyclodextrin – grafted– N-maleoyl chitosan nanoparticles	23-65	28-38 (after 8h, pH 6.8) 35-48 (after 24h, pH 6.8)	-59
Chitosan/PVA microsponge	45-79	3 (after 2h, pH 1.2) 25-30 (after 8h, pH 7.4) 51-71 (after 12h, pH 7.4)	-60

Table 4. Experimental ZP, PS, PDI and EE% of the prepared KP-loaded formulations.

Formulation code	ZP(mV)	PS (nm)	PDI	EE%
CHNP**(0%KP)**	+28.1 ±0.58	196.5 ±69	0.123	-----
CHNP/CNC**(0%)-F1**	+32.38 ±0.36	227.6 ±98.1	0.186	79.78 ± 2.11
CHNP/CNC**(2.5%)-F2**	+31.73 ±0.52	205.3 ±89.4	0.185	77.59 ± 1.95
CHNP/CNC**(5%)-F3**	+32.86 ±0.29	216.5 ±91.7	0.192	78.31 ± 3.15
CHNP/CNC**(10%)-F4**	+33.70 ±1.02	214.9 ±93.5	0.189	76.84 ± 2.86
CHNP/CNC**(20%)-F5**	+26.58 ±0.43	234.4 ±110	0.22	73.61 ± 3.45
CHNP/OXCNC**(2.5%)-F6**	+30.95 ±0.48	203.8 ±72.3	0.182	74.95 ± 2.76
CHNP/OXCNC**(5%)-F7**	+30.71 ±0.33	198.5 ±86.1	0.179	74.78 ± 3.35
CHNP/OXCNC**(10%)-F8**	+30.62 ±0.38	197.8 ±82.7	0.175	74.46 ± 3.51
CHNP/OXCNC**(20%)-F9**	+23.50 ±0.69	231 ±112.6	0.238	72.63 ± 4.37
CHNP/ACNC**(2.5%)-F10**	+33.19 ±0.36	212 ±98.5	0.193	76.32 ± 2.53
CHNP/ACNC**(5%)-F11**	+32.94 ±0.62	220 ±87.6	0.18	75.12 ± 1.95
CHNP/ACNC**(10%)-F12**	+33.81 ±0.16	225 ±108.5	0.183	75.45 ± 1.69
CHNP/ACNC**(20%)-F13**	+26.70 ±0.93	235 ±100.6	0.232	74.58 ± 2.39

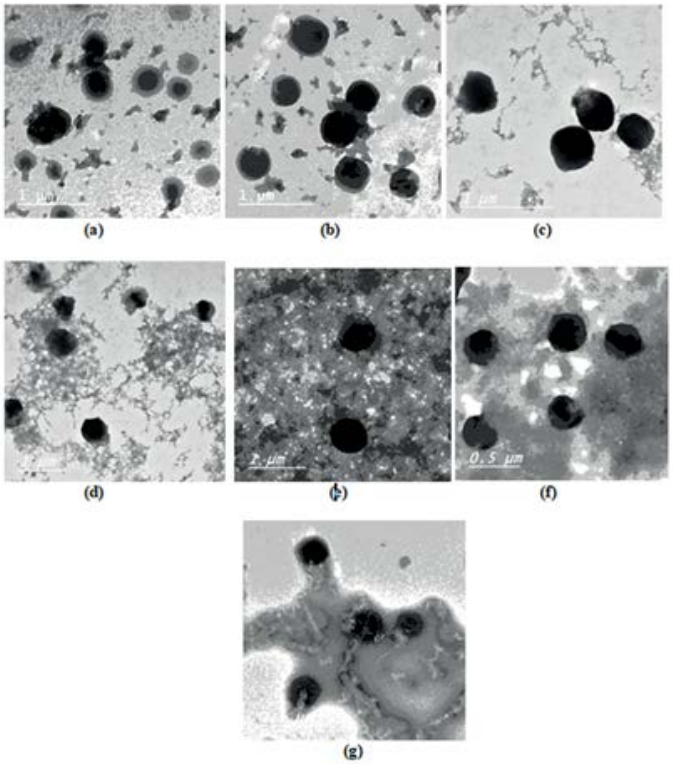

Figure 4. TEM images of (**a**) CHNP/CNC**(0%)-F1**, (**b**) CHNP/CNC**(10%)-F4**, (**c**) CHNP/CNC**(20%)-F5**, (**d**) CHNP/OXCNC**(10%)-F8**, (**e**) CHNP/OXCNC**(20%)-F9**, (**f**) CHNP/ACNC**(10%)-F12** and **(g)** CHNP/ACNC**(20%)-F13**.

FTIR spectra of KP-loaded nanocomposites

The possibility of interaction between the KP and CNC, OXCNC, ACNC or CHNP can be investigated from studying of FTIR spectra of CNC, OXCNC and ACNC (Figure 1c), and thus of KP, CHNP, CHNP/CNC **(10%)-F4**, KP-CHNP/OXCNC **(10%)-F8** and KP-CHNP/ACNC **(10%)-F12** (Figure 5). FTIR of pure KP (Figure 4a) showed the characteristic peaks at 2978.5–2933.2 cm^{-1} due to the aromatic C–H and carboxylic acid O–H stretching vibrations, 1652.7 cm^{-1} and 1697 cm^{-1} due to the ketonic carbonyl and carboxyl carbonyl stretching, respectively. The peak at 1595.8 cm^{-1} is corresponding to the aromatic C=C stretching, while peak at 1474.3 cm^{-1} is due to CH–CH_3 deformation. The peak at 2731 cm^{-1} is due to the C–H stretching and O–H deformation, and peak at 1697 cm^{-1} for the carboxylic O–H out of plane deformation. IR spectra range of 863–641 cm^{-1} for C–H out of plane deformation indicated the presence of aromatic ring [62].

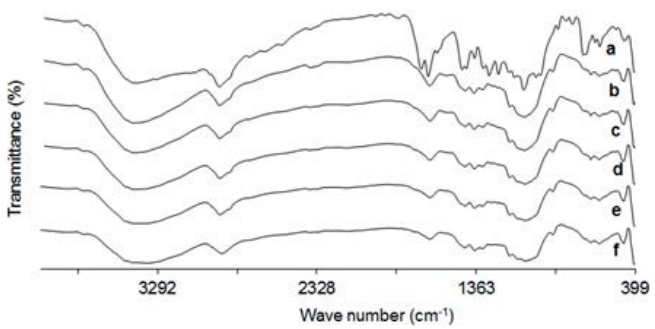

Figure 5. FTIR spectrum of a) KP, b) CHNP, c) CHNP/CNC(10%)-$\mathbf{F_4}$, d) CHNP/OXCNC(10%)-$\mathbf{F_8}$, e) CHNP/OXCNC(10%)-$\mathbf{F_{12}}$ and f) CNC.

CHNP, CNC, OXCNC and ACNC have nearly similar FTIR spectra due to the resemblance in their chemical structure and functional groups. FTIR spectrum of CHNP (Figure 4b) showed a broad band ranged between 3000–3700 cm^{-1} due to O–H and N–H stretching vibrations. Peak at 2800–3000 cm^{-1} is due to the C–H stretching vibrations, while peak at 1648 cm^{-1} is due to the amide C=O stretching vibrations. Peaks at 1425 cm^{-1} and 1558 cm^{-1} are due to NH_2 group, while peak at 1080 cm^{-1} is due to C-N stretching vibrations. Peak at 890-1147 cm^{-1} is due to the ether bonding [63].

FTIR spectrum of KP -CHNP/CNC (Figure 4c) showed the characteristic peaks of CNC, and CHNP, while that of KP-CHNP/OXCNC (Figure 4d) showed the characteristic peaks of OXCNC, and CHNP, and KP-CHNP/ACNC (Figure 4e) showed the characteristic peaks of ACNC, and CHNP. The peaks related to KP structure were at the same regions of CNC, OXCNC ACNC and CHNP and thus could not be seen separately. Absence of the interfering peaks emphasized that there were no unwanted chemical reactions between the KP and the other components. A small shift in the position of some of the peaks of the individual components was found in the prepared nanocomposites nanoparticles as a function of hydrogen bonding between the KP and the other composite components. For example, the amide carbonyl stretching vibration peak of chitosan at 1648 cm^{-1} was shifted to 1636 cm^{-1}, 1632 cm^{-1}, 1635 cm^{-1} due to the presence of CNC, OXCNC and ACNC, respectively, in addition to KP.

XRD of KP-loaded nanocomposites

XRD patterns of KP/CHNP and selected samples of KP-loaded nanocomposites with cellulose nanocrystals were studied and compared with that of CHNP to investigate the effect of the presence of KP and cellulose nanocrystals on the supramolecular structure of the cross-linked chitosan nanoparticles (Figure 6). Broad diffraction pattern with unresolved peaks was observed for CHNP (Figure 5a) due to their amorphous structure as a result of crosslinking of the chitosan chains using tripolyphosphate [64,65]. The broad pattern extended from 2θ angle of 10° to 30° and the peaks were centered at angles of about 11.6°, 18.3°, and 23.6°. Addition of KP had no effect on the diffraction pattern of CHNP (Figure 5b); that is indicated the efficient entrapment of KP into the cross-linked chitosan chains and absence of any chemical reactions between them. Addition of CNC, OXCNC or ACNC had no significant effect on the XRD pattern of CHNP except the peak at 2θ angle of 23.6° became sharper (Figure 5c-e), since the cellulose nanocrystals have XRD peaks (two major peaks centered at 2θ angles of 23° and 15°) in the same regions of CHNP peaks.

Conclusions

Cellulose Nanocrystals (CNC) isolated from date palm stalks by sulfuric acid hydrolysis, Oxidized Cellulose Nanocrystals (OXCNC) and Amine-Functionalized Cellulose Nanocrystals (ACNC) were merged with Chitosan Nanoparticles (CHNP) to control the release rate of KP developing a controlled drug release system. TEM images showed that the chemical modification either by oxidation or etherification with amine moiety had no significant effect on the CNC dimen-

Citation: Abo-Elseoud WS, Hassan ML, Sabaa MW, Basha M, Hassan EA, et al. (2020) Use of cellulose nanocrystals in chitosan nanoparticles carrier system for the controlled release of Ketoprofen. OSP J Nano med tech 1. JNN-1-101

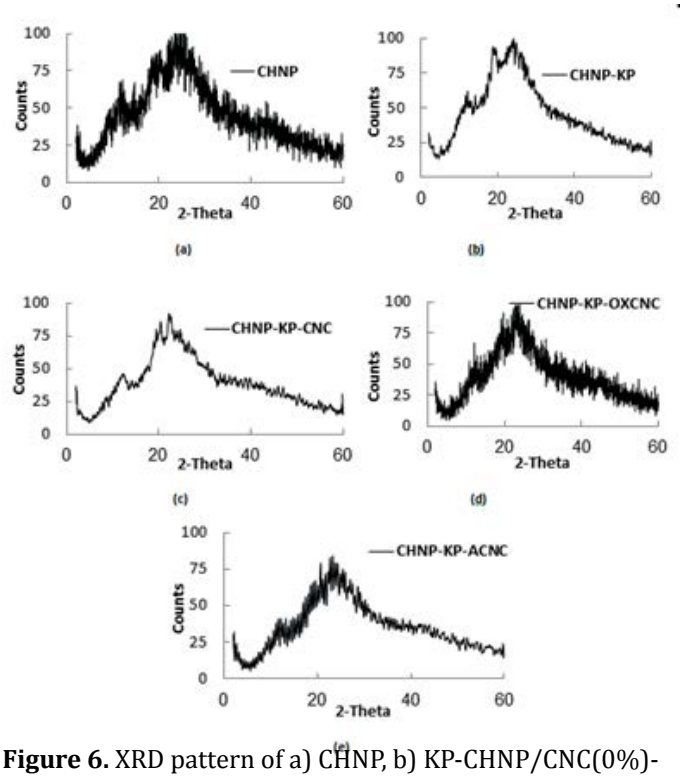

Figure 6. XRD pattern of a) CHNP, b) KP-CHNP/CNC(0%)-$\mathbf{F_1}$, c) KP-CHNP/CNC(10%)-$\mathbf{F_4}$, d) KP-CHNP/OXCNC(10%)-$\mathbf{F_8}$ and e) KP-CHNP/ACNC(10%)-$\mathbf{F_{12}}$.

sions. KP-loaded CHNP/CNC, CHNP/OXCNC and CHNP/ACNC nanoparticles were successfully prepared and characterized by high entrapment efficiency. Hydrogen bonding between CNC, OXCNC or ACNC and KP resulted in retarding its release from the prepared formulations producing a sustained and controlled release profile. KP-loaded CHNP/CNC formulations produced more sustained release profile of KP than that of both CHNP/OXCNC and CHNP/ACNC formulations; but all systems had more sustained release than that consists of neat CHNP. FTIR spectra showed no interaction between the KP and the other ingredients (CHNP and cellulose nanocrystals) of the prepared systems. Addition of KP to CHNP had no effect on its XRD pattern indicating that the entrapment of KP between the cross-linked chitosan chains and absence of chemical reaction between them. The prepared KP-CHNP/CNC, KP-CHNP/OXCNC, KP-CHNP/ACNC systems showed good drug release profile suitable for use as anti-inflammatory controlled-release drug systems.

References

1. Meyer M, Persson O (1998) Nanotechnology-interdisciplinarity, patterns of collaboration and differences in application. Scientometrics. 42: 195-205. [Crossref]
2. Gref R, Minamitake Y, Peracchia MT, Trubetskoy VS, Torchilin VP, et al. (1994) Biodegradable long-circulating polymeric nanospheres. Sci. 263: 1600-1603. [Crossref]
3. Elzoghby AO, Samy WM, Elgindy NA (2012) Albumin-based nanoparticles as potential controlled release drug delivery systems. J Control Release. 157: 168-182. [Crossref]
4. Jackson JK, Letchford K, Wasserman BZ, Ye L, Hamad WY, et al. (2011) The use of nanocrystalline cellulose for the binding and controlled release of drugs. Int J Nanomedicine. 6: 321-330. [Crossref]
5. Springate CM, Jackson JK, Gleave ME, Burt HM (2008) Clusterin antisense complexed with chitosan for controlled intratumoral delivery. Int J Pharm. 350: 53-64. [Crossref]
6. Dong S, Hirani AA, Colacino KR, Lee Y W, Roman M (2012) Cytotoxicity and cellular uptake of cellulose nanocrystals. Nano Life. 3: 1241006. [Crossref]
7. Mahmoud KA, Mena JA, Male KB, Hrapovic S, Kamen A, et al. (2010) Effect of surface charge on the cellular uptake and cytotoxicity of fluorescent labeled cellulose nanocrystals. ACS Appl Mater Interfaces. 2: 2924-2932. [Crossref]
8. Mosmann T (1983) Rapid colorimetric assay for cellular growth and survival: Application to proliferation and cytotoxicity assays. J Immunol Methods. 65: 55-63. [Crossref]
9. Roman M, Dong S, Hirani A, Lee YW (2009) Cellulose Nanocrystals for Drug Delivery. Polysaccharide Materials: Performance by Design. 1017: 81-91. [Crossref]
10. Pachuau L (2017) Application of nanocellulose for controlled drug delivery, chapter 1, Nanocellulose and nanohydrogel Matrices: biotechnological and biomedical applications. [Crossref]
11. Mendes BB, Domingues RM, Costa-Almeida R, Babo PS, Reis RL, et al. (2017) Injectable platelet lysate/cellulose nanocrystals hydrogels: a novel combined approach for regenerative medicine strategies. EUR CELLS MATER 33: 1473-2262. [Crossref]
12. Guo R, Lan Y, Xue W, Cheng B, Zhang Y, et al. (2017) Collagen-cellulose nanocrystal scaffolds containing curcumin-loaded microspheres on infected full-thickness burns repair. J Tissue Eng Regen M. [Crossref]
13. Akhlaghi SP, Berry RC, Tam KC (2013) Surface modification of cellulose nanocrystal with chitosan oligosaccharide for drug delivery applications. Cellulose. 30: 1747-1764. [Crossref]
14. Grishkewich N, Mohammed N, Tang J, Tam KC (2017) Recent advances in the application of cellulose nanocrystals. Curr Opin *Colloid* In. 29: 32-45. [Crossref]
15. Kovacs T, Naish V, O'Connor B, Blaise C, Gagné F, et al. (2010) An Ecotoxicological Characterization of Nanocrystalline Cellulose. *Nanotoxicology.* 4: 255-270. [Crossref]
16. Drogat N, Granet R, Sol V, Memmi A, Saad N, et al. (2011) Antimicrobial silver nanoparticles generated on cellulose nanocrystals. J Nanopart Res. 13: 1557-1562. [Crossref]
17. Singla R, Soni S, Padwad YS, Acharya A, Yadav SK (2017) Sustained delivery of BSA/HSA from biocompatible

plant cellulose nanocrystals for in-vitro cholesterol release from endothelial cells. Int J Biol Macromol. 104: 748-757. [Crossref]

18. Zainuddin N, Ahmad I, Kargarzadeh H, Ramli S (2017) Hydrophobic kenaf nanocrystalline cellulose for the binding of curcumin. Carbohydr Polym. 163: 261-269. [Crossref]

19. Muzzarelli RAA (1977) Chitin. 1-37. Pergamon Press, New York. [Crossref]

20. Roberts GAF (1992) Chitin Chemistry 1: 274-315. The Mac Millan Press, London. [Crossref]

21. Shao Y, Li L, Gu X, Wang L, Mao S (2015) Evaluation of chitosan-anionic polymers based tablets for extended-release of highly water-soluble drugs. Asian J Pharm Sci. 10: 24-30. [Crossref]

22. Garcia-Fuentes M, Alonso MJ (2012) Chitosan-based drug nanocarriers: Where do we stand? J Control Release.161: 496-504. [Crossref]

23. Hamidi M, Azadi A, Rafiei P (2008) Hydrogel nanoparticles in drug delivery. Adv Drug Deliv Rev. 60: 1638-1649. [Crossref]

24. Wang H (2009) Chitosan - cellulose nanocrystal polyelectrolyte complex particles: preparation, characterization, and in-vitro drug release properties. PhD thesis, Virginia Polytechnic Institute and State University, Blacksburg, Virginia. [Crossref]

25. Hirohata M, Ono K, Morinaga A, Yamada M (2008) Non-steroidal anti-inflammatory drugs have potent anti-fibrillogenic and fibril-destabilizing effects for a-synuclein fibrils *in-vitro*. Neuropharmacology. 54: 620-627. [Crossref]

26. Weder JE, Dillon CT, Hambley TW, Kennedy BJ, Lay PA, et al (2002) Copper complexes of non-steroidal anti-inflammatory drugs: an opportunity yet to be realized, Coord Chem Rev. 232: 95-126. [Crossref]

27. Habib MJ, Mesue R (1995) Development of controlled release formulations of ketoprofen for oral use. Drug Dev Ind Pharm. 21: 1463-1472. [Crossref]

28. Palmieri GF, Bonacucina G, Martino PD, Martelli S (2002) Microencapsulation of semisolid ketoprofen/polymer microspheres. Int J Pharm. 242: 175-178. [Crossref]

29. Sari R, Magda M, WINI Lestari W, Syamsur MAR (2015) Ketoprofen-carboxymethyl chitosan microparticles prepared by spray draying: optimization and evaluation. *Asian* J Pharm Clin Res. 8: 331-333. [Crossref]

30. Hardi J, Sugita P, Ambarsari L (2013) Dissolution behavior, stability and anti-inflammatory activity of ketoprofen coated tripolyphosphate modified chitosan nanoparticle. Indones J Chem. 13: 149-157. [Crossref]

31. Wagh P, Naik J (2015) Formulation and characterization of ketoprofen embedded polycaprolactone microspheres using solvent evaporation method. Admet & Dmpk. 3: 141-153. [Crossref]

32. Vueba ML, Batista de Carvalho LAE, Veiga F, Sousa JJ, et al. (2013) *In vitro* release of ketoprofen from hydrophilic matrix tablets containing cellulose polymer mixtures. Drug Dev Ind Pharm. 39: 1651-1662. [Crossref]

33. Shivakumar HN, Suresh S, Desai BG (2006) Design and Evaluation of Controlled Onset Extended Release Multiparticulate Systems for Chronotherapeutic Delivery of Ketoprofen. Indian J Pharm Sci. 68: 76-82. [Crossref]

34. Abo EL-Seoud WS, Hassan ML, Sabaa MW, Basha M, Hassan EA, et al. (2018) Chitosan nanoparticles/cellulose nanocrystals nanocomposites as a carrier system for the controlled release of repaglinide. Int J Biol Macromol. 111: 604-613. [Crossref]

35. Hassan ML, Bras J, Hassan EA, Silard C, Mauret E (2014) Enzyme-assisted isolation of microfibrillated cellulose from date palm fruit stalks. Ind Crop Prod. 55: 102-108. [Crossref]

36. Browning BL (1967) Methods of wood chemistry. *Interscience:* New York, 2. [Crossref]

37. Habibi Y, Chanzy H, Vignon MR (2006) TEMPO-mediated surface oxidation of cellulose whiskers. Cellulose. 13: 679-687. [Crossref]

38. Porath J, Fornstedt NJ (1970) Group fractionation of plasma proteins on dipolar ion exchangers. J Chromatogr. 51: 479-489. [Crossref]

39. Calvo P, RemunanLopez C, Vila-Jato JL, Alonso MJ, Remuñan-López C, et al. (1997) Chitosan and chitosan ethylene oxide propylene oxide block copolymer nanoparticles as novel carriers for proteins and vaccines. Pharm Res. 14: 1431-1436. [Crossref]

40. Sidiras DK, Koullas DP, Vgenopoulos AG, Koukios EG (1990) Cellulose crystallinity as affected by various technical processes. Cell Chem Technol. 24: 309-317. [Crossref]

41. Souto EB, Wissing SA, Barbosa CM, Muller RH (2004) Development of a controlled release formulation based on SLN and NLC for topical clotrimazole delivery. Int J Pharm. 278: 71-77. [Crossref]

42. Akhlaghi SP, Zaman M, Mohammed N, Brinatti C, Batmaz R, et al. (2015) Synthesis of amine functionalized cellulose nanocrystals: optimization and characterization. Carbohydr Res. 409: 48-55. [Crossref]

43. Zugenmaier P (2008) 'Crystalline cellulose and derivatives', in Timell, T.E. and Wimmer, R.W. (Eds.): Crystalline Cellulose and Cellulose Derivatives. Characterization and Structure, Springer-Verlag, Berlin, Heidelberg. 1-281. [Crossref]

44. Abou-Zeid R, Hassan EA, Bettaieb F, Khiari R, Hassan ML (2015) Use of cellulose and oxidized cellulose nanocrystals from olive stones in chitosan bionanocomposites. J Nanomater. 687490. [Crossref]

45. Filpponen I, Sadeghifar H, Argyropoulos DS (2011) Photoresponsive cellulose nanocrystals. Nanomaterials and

Nanotechnology. 1: 34-43. [Crossref]

46. Ivanova NV, Korolenko EA, Korolik EV, Zhbankov RG (1989) IR spectrum of cellulose. J Appl Spectrosc. 51: 847-851. [Crossref]

47. Silverstein RM, Bassler GC, Morrill TC (1981) Spectrometric identification of organic compounds. New York: John Wiley and Sons 4: QD272.S6 S55 [Crossref]

48. Dong S, Roman M (2007) Fluorescently labelled cellulose nanocrystals for bioimaging applications. J Am Chem Soc. 129: 13810-13811. [Crossref]

49. Azzam F, Heux L, Putaux JL, Jean B (2010) Preparation by grafting onto, characterization, and properties of thermally responsive polymer-decorated cellulose nanocrystals. Biomacromolecules. 11: 3652-3659. [Crossref]

50. Rodrigues S, Da Costa AMR, Grenha A (2012) Chitosan/carrageenan nanoparticles: Effect of cross-linking with tripolyphosphate and charge ratios. Carbohydr Polym. 89: 282- 289. [Crossref]

51. Wahyono D (2010) Characterization of chitosan nanoparticles and its effects to particle size and ketoprofen encapsulation efficiency. Master thesis, Bogor Agricultural University, Bogor, Indonesia. [Crossref]

52. Sugita P, Ambarsari L, Farichah F (2013a) Increasing amount and entrapment efficiency of chitosan-ketoprofen nanoparticle using ultrasonic method with varied time and amplitude. Int j recent res appl Stud. 14: 612-618. [Crossref]

53. Sugita P, Ambarsari L, Sari YA, Nugraha Y (2013b) Ketoprofen encapsulation optimization with chitosan-alginate cross-linked with sodium tripolyphosphate and its release mechanism determination using in-vitro dissolution. Int j recent res appl Stud. 14: 141-149. [Crossref]

54. Chimsook T (2013) Controlled release behaviors of ketoprofen from matrix polymer of chitosan and poly(ethylene glycol). Adv Mater Res. 813: 399-402. [Crossref]

55. Woraphatphadung T, Sajomsang W, Rojanarata T, Akkaramongkolporn P, Ngawhirunpat T, et al. (2017) Preparation and characterization of N-benzyl-N,O-succinyl chitosan polymeric micelles for solubilization of poorly soluble non-steroidal anti-inflammatory drugs. Trop J Pharm Res. 16: 2349-2357. [Crossref]

56. Medeiros SF, Fonseca JM, Alves GM, Santos DM, Campana-Filho SP, et al (2018) Poly(N-vinylcaprolactam-co-itaconic acid-co-ethylene glycol dimethacrylate)-based microgels embedded in chitosan matrix for controlled release of ketoprofen. International Journal of Biomedical and Biological Engineering. 12. [Crossref]

57. Lins LC, Bazzo GC, Barreto PLM, Pires ATN (2014) Composite PHB/chitosan microparticles obtained by spray drying: effect of chitosan concentration and crosslinking agents on drug release. J Braz Chem Soc. 25: 1462-1471. [Crossref]

58. Sugita P, Ambarsari L, Lidiniyah. (2015) Optimization of ketoprofen-loaded chitosan nanoparticle ultrasonication process. *Procedia Chem*. 16: 673-680. [Crossref]

59. Hou J, Yu X, Shen Y, Shi Y, Su C, et al. (2017) Triphenyl Phosphine-Functionalized Chitosan Nanoparticles Enhanced Antitumor Efficiency Through Targeted Delivery of Doxorubicin to Mitochondria. *Nanoscale* Res Lett. 12: 158. [Crossref]

60. Rathore C, Jain N, Garg N, Mahindroo N, Sharma G, et al. (2017) Polysaccharide-microsponge based matrix tablet for colon targeting of ketoprofen: *in-vitro* and *in vivo* evidence. Int j pharm sci res. 8: 4250 - 4260. [Crossref]

61. Wu L, Zhang J, Watanabe W (2011) Physical and chemical stability of drug nanoparticles. Adv Drug Deliv Rev. 63: 456-469. [Crossref]

62. Grimling B, Górniak A, Meler J, Szcześniak M, Pluta J (2014) Characterization and dissolution properties of ketoprofen in binary solid dispersion with chitosan. Progress on Chemistry and Application of Chitin and Its Derivatives XIX. 15-22. [Crossref]

63. De Mesquita JP, Donnici CL, Pereira FV (2010) Biobased nanocomposites from layer-by-layer assembly of cellulose nanowhiskers with chitosan. Biomacromolecules. 11: 473-480. [Crossref]

64. Bhumkar DR, Pokharkar VB (2006) Studies on effect of pH on cross-linking of chitosan with sodium tripolyphosphate: a technical note. AAPS PharmSciTech. 7: 138-143. [Crossref]

65. Wan Y, Creber KAM, Peppley B, Bui VT (2003) Synthesis, characterization and ionic conductive properties of phosphorylated chitosan membranes. Macromol Chem Phys. 204: 850-858. [Crossref]